Proximity Relationships within the Fc Segment of Rabbit Immunoglobulin G Analyzed by Resonance Energy Transfer†

Robert Luedtke, Charles S. Owen,‡ Jane M. Vanderkooi, and Fred Karush*

ABSTRACT: Resonance energy transfer analysis has been carried out with a noncovalent rabbit hybrid of immunoglobulin G (IgG) composed of normal rabbit IgG and rabbit anti-lactose IgG. The hybrid IgG was prepared from proteins in which the single inter-heavy-chain disulfide linkage was specifically reduced and alkylated. Normal rabbit IgG was alkylated with the iodoacetyl derivative of *N*-(aminoethyl)-5-naphthylamine-1-sulfonic acid while the rabbit anti-lactose IgG was alkylated with either iodoacetamide or the iodoacetyl derivative of *p*-[[*p*-(dimethylamino)phenyl]azo]aniline. Fractionation with an anti-lactose-specific immunoadsorbent yielded a population in which each fluorescent donor [*N*-[(acetylamino)ethyl]-5-naphthylamine-1-sulfonic acid] was adjacent to a nonfluorescent acceptor [*N*-acetyl-*p*-[[*p*-(dimethylamino)phenyl]azo]aniline]. Data on fluorescence quantum yield, excited-state lifetime, time-resolved emission anisotropy, and steady-state fluorescence polarization revealed a distribution of distances between the donor and acceptor. In the native molecule, the hinge regions are known to be covalently linked by a single disulfide bond. In the absence of this linkage, the hinge regions were separated such that for a majority of the molecules in solution (~60%) the separation was 50–60 Å. In the context of current knowledge of the IgG molecule, it is evident that the principle forces maintaining the integrity of the native, functional Fc segment are the strong noncovalent interactions of the C_H3 domains and the single inter-heavy-chain disulfide bond.

There is extensive evidence in support of the current concept that the immunoglobulin molecule is structurally and functionally segregated into a series of sequence homology regions termed domains. DNA sequence analysis of mouse immunoglobulin genes has established that each domain, as well as the hinge region, is encoded by a discrete segment of DNA (Sakano et al., 1979). Protein sequence and X-ray crystallographic analyses have demonstrated that each domain is comprised of approximately 110 amino acid residues, possesses at least one intrachain disulfide bond, and is folded into two layers of anti-parallel β-pleated sheets (Dorrington, 1978; Davies et al., 1975; Poljak, 1975). Furthermore, each domain of immunoglobulin G (IgG) is associated with a complementary domain on a separate chain by a disulfide bond and/or noncovalent interactions across an apolar interface to form a modular organizational unit. X-ray crystallographic analysis of the Fc fragment of human IgG1 indicates that the module comprised of the second constant domains (C_H2–C_H2) is unique in that the domains do not interact. Noncovalent association of the C_H2 domains is apparently prevented by the disposition of the carbohydrate chains, which are rigidly attached to the interface between the C_H2 domains (Deisenhofer et al., 1976). The hinge disulfide(s) and the strong noncovalent associations of the third constant domains, C_H3, of IgG appear to be the predominant structures which maintain the C_H2 domains in close proximity and stabilize the native conformation of the Fc segment.

There are several biological and biophysical observations which indicate that the hinge disulfide bond(s) is(are) essential to the stability of a native, functional Fc segment. Upon mild reduction and alkylation, the ability of rabbit IgG to induce cytotoxicity in concert with human lymphocytes was diminished, although this modified IgG was able to inhibit the cytotoxicity induced by native IgG (Michaelsen et al., 1975). Inhibition of the binding of rabbit anti-HSA/HSA[1] complexes to macrophages was shown to be greater for intact rabbit IgG than for the mildly reduced and alkylated protein (Arend & Mannik, 1972). The reactivity of rabbit and human IgG with the C1 component of complement has been shown to be dependent upon an intact hinge disulfide. On the other hand, the Fc fragment from human IgG also could bind C1, but its activity was shown to be insensitive to the presence or absence of intact hinge disulfides. Similarly, mildly reduced and alkylated human IgG1 and its Fc fragment showed a diminution of its ability to bind human placental plasma membrane vesicles when compared to the unmodified species (Van Der Meulen et al., 1980).

No alterations in the structure either of IgG or of its antigen combining site have been observed by circular dichroism or optical rotatory dispersion following mild reduction (Bjork & Tanford, 1971; Stevenson & Dorrington, 1970; Azuma et al., 1974; Rockey et al., 1972). However, a comparison of time-dependent fluorescence polarization of DNS-lysine bound to rabbit anti-DNS IgG indicated greater rotational freedom for the mildly reduced form than for the native molecule (Chan & Cathou, 1977). In addition, a comparison of hydrogen–deuterium exchange for native and mildly reduced and alkylated forms of a human myeloma IgG1 indicated an increase in the molecular conformational mobility with a decrease in the free-energy barrier to solvent exposure for the modified

† From the Departments of Microbiology (R.L. and F.K.) and Biochemistry and Biophysics (J.M.V.), University of Pennsylvania School of Medicine, Philadelphia, Pennsylvania 19104, and the Department of Biochemistry (C.S.O.), Thomas Jefferson University, Jefferson Medical College, Philadelphia, Pennsylvania 19107. *Received October 13, 1980.* This study was supported by U.S. Public Health Service Research Grant AI-09492 from the National Institute of Allergy and Infectious Diseases.

* Correspondence should be addressed to this author. He is a recipient of U.S. Public Health Service Research Career Award 5 K6 AI-14012 from the National Institute of Allergy and Infectious Diseases.

‡ Recipient of U.S. Public Health Serivce Research Career Development Award GN-00318 from the National Institute of General Medical Sciences.

[1] Abbreviations used: AEDANS, *N*-[(acetylamino)ethyl]-5-naphthylamine-1-sulfonic acid; DAAzo, *N*-acetyl-*p*-[[*p*-(dimethylamino)phenyl]azo]aniline; IAA, iodoacetamide; I-1,5-AEDANS, *N*-[[(iodoacetyl)amino]ethyl]-5-naphthylamine-1-sulfonic acid; I-DAAzo, *N*-(iodoacetyl)-*p*-[[*p*-(dimethylamino)phenyl]azo]aniline; DNS, 5-(dimethylamino)-1-naphthalenesulfonyl; HSA, human serum albumin.

0006-2960/81/0420-2927$01.25/0

species (Venyaminov et al., 1976). Finally, Romans and coworkers (1977) hypothesized that upon mild reduction and alkylation of human IgG the C_H2 domains spontaneously dissociate, each domain gains independent modes of movement, and the molecule acquires additional segmental flexibility. Their experiments involved the conversion by mild reduction of "incomplete" or nonagglutinating human alloantibodies to direct agglutinins. This result was attributed to the conversion of the IgG molecule to a configuration which permitted cell bridging due to an increase in the distance which the modified immunoglobulin could span.

This paper presents the findings of a resonance energy transfer study designed to define the spatial relationship of the C_H2 domains of midly reduced and alkylated rabbit IgG. A population of noncovalently hybridized rabbit IgG was prepared from normal rabbit IgG and rabbit anti-lactose IgG. The single inter-heavy-chain disulfide bond of the former was reduced and alkylated with a reagent which contained a fluorescent energy donor. The alkylating reagent for the latter contained an acceptor (sample hybrid) or was iodoacetamide (control hybrid). The quantum yield and excited-state lifetime of the donor fluorophore in the absence or presence of the acceptor were compared in order to quantitate the efficiency of energy transfer and, thereby, determine the apparent distance between the C_H2 domains in the mildly reduced and alkylated species. The results demonstrated that the mildly reduced and alkylated hybrid rabbit IgG was not in a native quaternary configuration. The results are analyzed and discussed in terms of a dynamic, flexible model for the immunoglobulin molecule.

Materials and Methods

Organic Synthesis. AEDANS Derivatives. *N*-[(Acetylamino)ethyl]-5-naphthylamine-1-sulfonic acid (AEDANS) was prepared by the procedure of Hudson & Weber (1973) with the modification that acetic anhydride (Baker), rather than *p*-nitrophenyl acetate, was used to acetylate *N*-(aminoethyl)-5-naphthylamine-1-sulfonic acid. *N*-[[(Iodoacetyl)amino]ethyl]-5-naphthylamine-1-sulfonic acid (I-1,5-AEDANS) was obtained commercially (Aldrich) and kept in the dark at −20 °C.

DAAzo Derivatives. *N*-Acetyl-*p*-[[*p*-(dimethylamino)phenyl]azo]aniline (DAAzo) was synthesized by reacting 240 mg (1.0 mmol) of *N*,*N*-dimethyl-4,4′-azodianiline (Eastman) with 1.0 mL of 10.6 M acetic anhydride (Baker) in 20 mL of ethyl acetate in the presence of 7.2 mmol of triethylamine. The reaction proceeded at room temperature for 12 h. Thin-layer chromatography (TLC) in either benzene or chloroform indicated complete acetylation. The reaction mixture was flash evaporated, and the residue was washed 5 times in 10 mL of cold isopropyl ether (0 °C). This residue was then dried at room temperature in vacuo. The molar extinction coefficients of DAAzo in 0.1 M Tris-HCl and 8.0 M urea at pH 8.0 are $\epsilon_{463} = 2.70 \times 10^4$ and $\epsilon_{280} = 7.21 \times 10^3$. Anal. Calcd for $C_{16}H_{18}N_4O$: C, 68.1; H, 6.4; N, 19.9. Found: C, 68.0; H, 6.5; N, 19.7.

N-(Iodoacetyl)-*p*-[[*p*-(dimethylamino)phenyl]azo]aniline (I-DAAzo) was synthesized by reacting 240 mg (1.0 mmol) of *N*,*N*-dimethyl-4,4′-azodianiline (Eastman) with 372 mg (2.0 mmol) of iodoacetic acid (Sigma) in the presence of 824 mg (4.0 mmol) of *N*,*N*′-dicyclohexylcarbodiimide (DCCI) with 15.0 mL of ethyl acetate in the dark for 3 h at room temperature. Because of the photolability of iodoacetyl derivatives, the following steps were also performed in the dark. Dicyclohexylurea (DCU) was removed by centrifugation and filtration of the supernate through glass wool. The supernate was flash evaporated, and the residue was suspended in 10 mL of cold isopropyl ether. The residue was washed 10 times with 10-mL volumes of cold isopropyl ether (0 °C) and dried in vacuo at room temperature. Thin-layer chromatography in chloroform indicated a major and a minor yellow component with R_f values of 0.35 and 0.0, respectively. Incubation of TLC plates (Eastman 13191 silica gel with fluorescent indicator) in an iodine chamber confirmed the removal of DCCI and DCU. A regimen of TLC indicator sprays was designed to detect the presence of reactive iodoacetyl compounds: (a) 0.04 M 2-mercaptoethanol, 0.1 M $NaHCO_3$, and 50% ethanol in H_2O (v/v) followed by drying; (b) 0.1 M *N*-ethylmaleimide (Sigma) in 95% ethanol followed by drying; and finally (c) 0.1 M $NaNO_2$, and 0.35 N HCl in stabilized starch indicator solution (Fisher). A blue color indicated the generation of iodine. Only the major component indicated a reactive iodoacetyl moiety. The TLC also provided verification of the effective removal of iodoacetic acid. A purity of 90% was assumed on the basis of elemental analysis. Anal. Calcd for $C_{16}H_{17}N_4OI$: C, 47.1; H, 4.2; N, 13.7; I, 31.1. Found: C, 48.7; H, 5.2; N, 12.1; I, 28.4.

Immunoglobulin Preparations. Normal rabbit IgG (Pentex) was stored as a lyophilized powder at −20 °C. Rabbit anti-lactose IgG was obtained from New Zealand white rabbits injected with *Streptococcus faecalis* (strain N) as described previously (Ghose & Karush, 1973). Immune serum was chromatographed on a *p*-aminophenyl-β-lactoside (PAPL) conjugated Sepharose 4B column (Lac–Sepharose). The anti-lactose-specific antibody was eluted with 0.2 M lactose in 0.01 M phosphate buffer, 0.15 M NaCl, and 0.01% NaN_3, pH 7.4. The antibody preparation was subsequently chromatographed on Sephadex G-200 in phosphate-buffered saline to select the IgG fraction. Concentrations of rabbit IgG were obtained from the optical density by using $E_{280nm}^{1\%,1cm} = 14.4$.

Noncovalent IgG Hybrid Formation. Rabbit IgG preparations were reduced and alkylated by using the following protocol. A solution of rabbit IgG (4.5–5.0 mg/mL) in 0.05 M Tris-HCl, pH 8.0, was reduced with a final concentration of 20 mM 2-mercaptoethanol for 60 min at room temperature under a nitrogen atmosphere. Glacial acetic acid was added to make a final concentration of 0.65 M. The sample was chromatographed on a Sephadex G-25 column (2 × 20 cm) and eluted with a 20 mM acetic acid and 1.0 mM EDTA solvent which had been degassed and bubbled with nitrogen for a minimum of 2 h prior to use (pH 3.5). The void volume peak was pooled and adjusted to pH 5.0 with 3.0 M Tris-HCl, pH 9.0. The appropriate alkylating reagent was added in darkness and the pH further adjusted to pH 8.0. The sample was then placed under a nitrogen atmosphere in the dark at room temperature with stirring. For iodoacetamide (IAA) and I-1,5-AEDANS, the alkylating reagent was used in 50% excess over the heavy-chain concentration for 90 min. For I-DAAzo, a 500% excess over the heavy-chain concentration was used for 20 h. Samples were then dialyzed extensively vs. 0.02 M Tris-HCl and 0.15 M NaCl, pH 8.0.

Prior to formation of rabbit noncovalent hybrid IgG, the normal rabbit IgG, which had been alkylated with I-1,5-AEDANS, was chromatographed on Sephadex G-100 in 0.01 M phosphate with 8.0 M urea at pH 7.2 in order to remove any reduced and alkylated light chains. A 100% excess of free rabbit light chains, previously alkylated with iodoacetamide, was added to the void volume peak prior to dialyzing vs. 0.02 M Tris-HCl, pH 8.0. For the formation of noncovalent hybrid molecules, normal rabbit IgG alkylated with I-1,5-AEDANS was mixed with either anti-lactose IgG alkylated with iodo-

acetamide or anti-lactose IgG alkylated with I-DAAzo. A ratio of normal rabbit IgG to anti-lactose IgG of 30:70 was used with a final total IgG concentration of approximatley 4.0 mg/mL. The pH was adjusted to 2.5 by addition of 1.2 N HCl, and the solution was incubated for 60 min. The pH was readjusted to 7.8 with 1.0 M Tris-HCl, pH 8.0, buffer and equilibrated for 60 min at room temperature (Hong & Nisonoff, 1965). Hybrid preparations were then chromatographed on a 20-mL column of Lac–Sepharose and washed with phosphate-buffered saline. Antibody possessing at least one lactose-specific combining site was eluted with 0.3 M lactose and dialyzed vs. 0.0 M Tris-HCl and 0.15 M NaCl, pH 8.0. The samples were then chromatographed on Sephadex G-200 in phosphate-buffered saline, pH 7.2, to select a nonaggregated four-chain component. Sodium dodecyl sulfate–polyacrylamide gel electrophoresis ($NaDodSO_4$–polyacrylamide gel electrophoresis) was carried out as previously described (Luedtke et al., 1980). Destained gels were scanned at 620 nm by using an ISCO Model 1310 gel scanner.

Spectral Analysis. Absorption spectra were obtained by using a Cary 15 spectrophotometer with samples at ambient temperature. Emission spectra for the determination of quantum yields were obtained by using a Perkin-Elmer Model 512 double-beam fluorescence spectrophotometer in the ratio mode with diffuse plates in the reference chamber. The relative quantum yield of the donor fluorophore was determined by the method of Parker et al. (1967) with AEDANS in 100% ethanol as a relative standard, assuming a quantum yield of 0.69 (Hudson & Weber, 1973). Comparisons were made by weighing the graphs of the relative corrected emission spectra as a function of the wavenumber. In order to compare donor quantum yield in the presence vs. absence of the acceptor, 400 μL of the appropriate hybrid IgG preparation was added to 500 μL of either 7.2 M guanidine-HCl or phosphate-buffered saline. For each hybrid preparation, the spectrum in the guanidine-HCl solvent was assumed to be free from the influence of the acceptor, due to the dissociation of the protein into half-molecules. Consequently, these spectra could be used to correct the donor emission scans in phosphate-buffered saline for differences in donor concentration.

Steady-state fluorescence polarization of the noncovalent hybrid rabbit IgG preparations for the purpose of quantitating energy transfer was performed by using an SLM Model 8000 photon counting fluorometer (SLM Instruments, Urbana, IL) equipped with an MC640/M double-grating excitation monochromator, an MC320/M single-grating emission monochromator, an LH450 xenon lamp, an R928/P Hamamatsu photomultiplier tube cooled to −20 °C, and a PC810 photon counting acquisition unit. The excitation wavelength was 330 nm with 16- and 8-nm slits, with the emission monitored at 500 nm by using a 16-nm slit. The integration time was 20 s. The temperature of a reference solution was monitored continuously by using a Bailey BAT-8C digital thermometer. The temperature was regulated by a water bath which circulated coolant through the metal block which held the sample and the reference cuvettes. The degree of polarization, P, was calculated from eq 1 where $I_{\parallel}$ and $I_{\perp}$ are the

$$P = \frac{I_{\parallel} - GI_{\perp}}{I_{\parallel} + GI_{\perp}} \tag{1}$$

relative intensities of the vertical and horizontal fluorescent components by using vertically polarized exciting light. G is the ratio of the vertical and horizontal fluorescent emission observed with horizontally polarized exciting light, and corrects for instrumental bias in detecting polarized light.

Fluorescence decay curves were obtained by the monophoton counting technique. The instrumentation has been described previously (Luedtke et al., 1980). The excitation flash was from a thyrotron gated arc through a 355 ± 40 nm filter. The emission filter was a 455-nm cutoff filter (Schott Optical Glass, Duryea, PA). The Laplace transform method of Gafni et al. (1975) was used to analyze the experimental data. The donor decay curve was analyzed to find the best fit by a two-exponential decay.

Time-resolved fluorescence anisotropy measurements were obtained by using the photon counting instrument. Unpolarized light was used for excitation, and a polarizer (Polacoat 4B) was inserted between the sample and the emission photomultiplier. The orientation of the polarizer was under computer control. Three decay profiles were obtained: the lamp profile, $G(t)$, and decay profiles with the polarizer parallel, $I_{\parallel}(t)$, or perpendicular, $I_{\perp}(t)$, to the normal of the plane formed by the lamp, sample, and detector.

The total fluorescence intensity is proportional to $D(t)$ where

$$D(t) = 2I_{\parallel}(t) + I_{\perp}(t) \tag{2}$$

The apparent anisotropy, $A(t)$, is given by eq 3. This definition (Wahl, 1975) yields values for the anisotropy which are pro-

$$A(t) = \frac{I_{\parallel}(t) - I_{\perp}(t)}{D(t)} \tag{3}$$

portional to those which would have been obtained from the same sample by the usual method with polarized exciting light, but the numerical values obtained from eq 2 and 3 are smaller by a factor of 0.5 in every case.

Analysis of Energy Transfer. The rate of electronic energy transfer (k_T) due to dipole–dipole interactions is given by eq

$$k_T = R^{-6}K^2Jn^{-4}(8.71 \times 10^{23}\ s^{-1}) \tag{4}$$

4 where R is the distance in angstroms between the centers of the donor and acceptor chromophores, n is the index of refraction of the medium between donor and acceptor, taken to be 1.4, and K^2 is the orientation factor for dipole–dipole transfer, which can theoretically vary from 0 to 4. The spectral overlap integral (J) is defined by eq 5 where λ is the wave-

$$J = \frac{\int F(\lambda)\epsilon(\lambda)\lambda^4\, d\lambda}{\int F(\lambda)\, d\lambda} \tag{5}$$

length, $F(\lambda)$ is the relative fluorescence intensity of the donor as a function of λ, and $\epsilon(\lambda)$ is the molar extinction coefficient of the acceptor as a function of λ (Stryer, 1978). Numerical values for J were obtained by digitizing the steady-state fluorescence emission spectrum of the donor and the absorption spectrum of the acceptor moiety by using the same HP 9825 calculator with 9872 plotter that was used in the analysis of the nanosecond decay curves.

The efficiency of energy transfer can be represented as eq 6 where R_0 is the distance in angstroms at which the probability of energy transfer equals the probability of excited-state

$$E = R^{-6}/(R^{-6} + R_0^{-6}) \tag{6}$$

decay by radiative or ratiationless processes and is given by eq 7 where Q is the donor fluorescence quantum yield in the

$$R_0 = (JK^2Qn^{-4})^{1/6}(9.7 \times 10^3) \tag{7}$$

absence of energy transfer.

Results

Chemical Modification of Rabbit IgG. Mildly reduced normal rabbit IgG was alkylated with I-1,5-AEDANS as

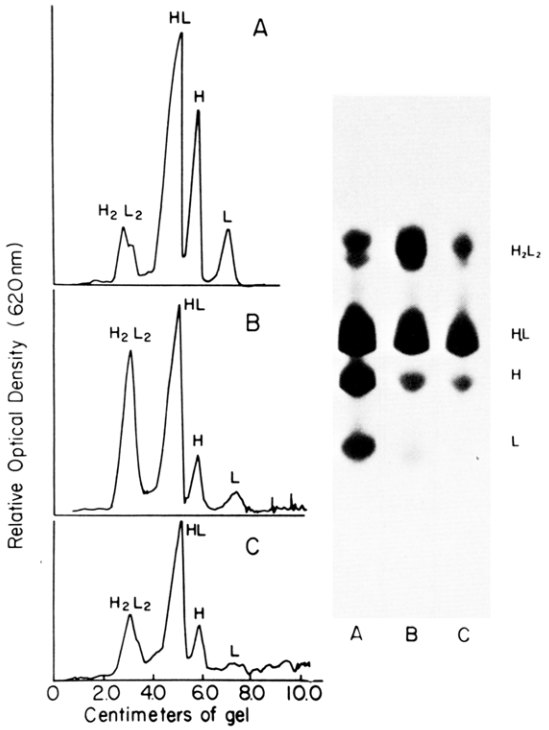

FIGURE 1: Stained $NaDodSO_4$–polyacrylamide gel electrophoresis tube gels (right) and linear scans of the gels (left) are shown of rabbit IgG after mild reduction and alkylation. (A) Rabbit anti-lactose IgG alkylated with iodoacetamide. (B) Rabbit anti-lactose IgG alkylated with I-DAAzo. (C) Normal rabbit IgG with I-1,5-AEDANS prior to chromatography with G-100 Sephadex in 0.01 M PO_4 and 8.0 M urea, pH 7.2.

described under Materials and Methods. In order to calculate the number of covalently linked AEDANS groups per IgG molecule, molar extinction coefficients of $\epsilon_{337} = 6 \times 10^3$ and $\epsilon_{280} = 1.26 \times 10^3$ were used for the AEDANS moiety (Hudson & Weber, 1973) while $E^{1\%,1cm}_{280nm} = 14.4$ was used for rabbit IgG. The optical density of the protein at 337 nm was found to be 2.5% of the 280-nm value. A value of 1.70 AEDANS per molecule of normal rabbit IgG was calculated.

Scans of the $NaDodSO_4$–polyacrylamide gel electrophoresis gels of normal rabbit IgG–AEDANS, shown in Figure 1, indicated that 25% of the protein remained in a covalently linked four-chain structure (H_2L_3) while 60% was covalently linked as half-molecules (HL). Visual examination of $NaDodSO_4$–polyacrylamide gel electrophoresis gels under ultraviolet light showed that the major fluorescent band was located at the HL position, with some fluorescence at the heavy-chain position. Upon complete reduction to heavy and light chains, only the heavy-chain position exhibited fluorescence. It was apparent, therefore, that the covalent AEDANS label was exclusively on the heavy chain.

Previous experiments had demonstrated that in the absence of a reducing reagent I-1,5-AEDANS, at concentrations 10-fold greater than those used here, labeled about 0.2 AEDANS per IgG. In addition, in the absence of an alkylating reagent, 100% of the heavy–light chain and 80% of the heavy–heavy chain interchain disulfide bonds were re-formed (Luedtke et al., 1980). It was concluded that alkylation of thiol groups predominated due to (1) the stronger nucleophilic character of the sulfhydryl group in comparison with other amino acid residues, (2) the minimization of the concentration of the alkylating reagent necessary to complete the modification by prior removal of the reducing agent by chromatography, (3) the conduction of the alkylation at pH 8.0, thereby avoiding the alkylation of lysine residues (Means & Feeney, 1971), and (4) the absence of extensive reoxidation of the inter-heavy-chain disulfide linkage. It was estimated that a minimum of 85% of the AEDANS molecules was covalently linked to cysteine-242,[2] which is the residue forming the inter-heavy-chain disulfide bond, with no more than 15% located at heavy-chain cysteine-127 (or -128), which forms the disulfide bond with the light chain (Fruchter et al., 1970).

Mildly reduced rabbit anti-lactose IgG was chemically modified with either iodoacetamide or I-DAAzo. The procedure for alkylation with iodoacetamide was similar to that used for I-1,5-AEDANS. Linear scans of $NaDodSO_4$–polyacrylamide gel electrophoresis gels (relative absorbance at 620 nm as a function of gel length) indicated that 10% of the protein remained in the H_2L_2 configuration (Figure 1). However, due to the low solubility of the I-DAAzo in aqueous medium, the alkylation step was performed as a heterogeneous reaction with a 500% excess of alkylating reagent over the heavy-chain concentration for an extended period of time (20 h). Linear scans of $NaDodSO_4$–polyacrylamide gel electrophoresis gels indicated that 35% of the protein remained in an H_2L_2 covalent state with 50% covalently linked as half-molecules (HL). A value of 1.8 covalent DAAzo groups per IgG was calculated by utilizing the extinction coefficients obtained for the model compound DAAzo in 0.1 M Tris-HCl and 8.0 M urea, pH 8.0. Fixation of $NaDodSO_4$–polyacrylamide gel electrophoresis gels in an acetic acid/ethanol/H_2O (14:40:160) solution with 10% trichloroacetic acid generated an intense reddish purple color characteristic of the protonated dimethylaminophenylazophenyl moiety. The DAAzo group was located predominantly at the HL position. Upon reduction to heavy and light chains, only the heavy chain visually appeared labeled. The number of DAAzo groups per half-molecule of anti-lactose was calculated to be 1.4/HL. This calculation excludes the unmodified H_2L_2 covalent species which was not involved in hybrid formation. For subsequent calculations, it was assumed, therefore, that all of the inter-heavy-chain disulfide-forming cysteines had been modified with DAAzo.

Noncovalent Hybrid Preparations. Two noncovalent hybrid rabbit IgG preparations were formed by acidification (Hong & Nisonoff, 1965). Hybrid A contained both a donor and an acceptor (normal rabbit IgG–AEDANS/anti-lactose–DAAzo), and hybrid C contained a donor in the absence of an acceptor (normal rabbit IgG–AEDANS/anti-lactose–IAA). For both hybrid preparations, approximately 81% of the total protein bound to the Lac–Sepharose immunoadsorbent (by OD_{280}). In addition, this fraction contained about 56% of the original fluorescence (measured by the relative fluorescence in 6.0 M guanidine-HCl with 330-nm excitation and 480-nm emission). After removal of lactose by dialysis, each sample was chromatographed on a Sephadex G-200 column in phosphate-buffered saline to select the nonaggregated four-chain structure (Figure 2). The samples were kept at 4 °C without further concentration in order to minimize the formation of soluble aggregates.

Energy Transfer Analysis. A quantum yield of 0.51 for AEDANS coupled to normal rabbit IgG was calculated by using AEDANS in 100% ethanol as a relative standard which had a quantum yield of 0.69 (Hudson & Weber, 1973). The emission spectrum of the probe was similar to that of AEDANS in 40% ethanol (quantum yield = 0.47), and its corrected emission maximum was 495 nm. Figure 3 shows the

[2] This number is based on the numbering system of Kabat et al. (1979).

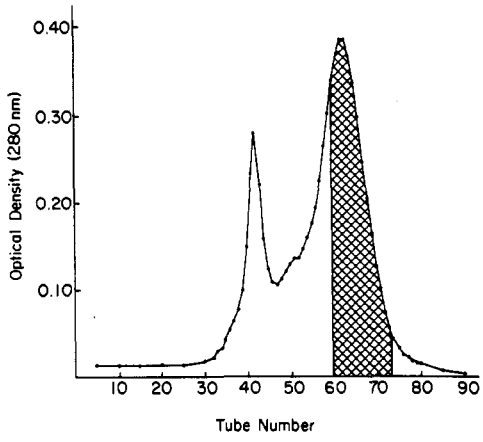

FIGURE 2: Hybrid C. Normal rabbit IgG–AEDANS/anti-lactose IgG–IAA chromatographed on G-200 Sephadex in phosphate-buffered saline (PBS), pH 7.2. Cross-hatching represents the tubes which were pooled and used for fluorescence analysis.

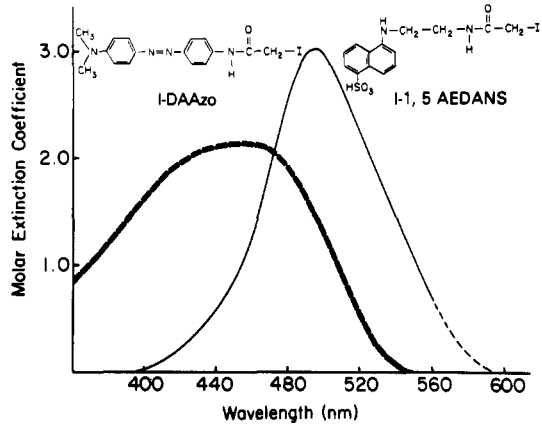

FIGURE 3: Absorption spectrum of rabbit anti-lactose IgG-DAAzo in PBS is shown (---) with the structure of the alkylating reagent, I-DAAzo, directly above. The corrected emission spectrum of normal rabbit IgG–AEDANS is shown (—) with the structure of the alkylating reagent, I-1,5-AEDANS, directly above. The emission was corrected to 560 nm. Values of R_0 = 40.8 Å and $J = 5.90 \times 10^{-14}$ cm^6/mmol were calculated for this donor–acceptor pair, assuming $K^2 = 0.67$, a quantum yield of 0.51 of the AEDANS moiety, and a molar extinction coefficient of 2.14×10^4 at 450 nm.

overlapping corrected emission spectrum of normal rabbit IgG–AEDANS and the absorption spectrum of anti-lactose–DAAzo. The DAAzo moiety shows a broad absorption peak from 430 to 450 nm in phosphate-buffered saline. When 0.1 M Tris-HCl and 8.0 M urea, pH 8.0, were used as the solvent system, an absorption peak from 455 to 493 nm was observed. A value of 40.8 Å for R_0 was calculated by using a molar extinction coefficient of 2.14×10^4 for the DAAzo coupled to anti-lactose IgG in phosphate-buffered saline at maximum absorption, a quantum yield of 0.51 for AEDANS coupled to normal rabbit IgG, an orientation factor of $K^2 = 0.67$, and an overlap integral of $J = 5.90 \times 10^{-14}$ cm^6/mmol.

In order to determine the efficiency of energy transfer between the donor (AEDANS) and the acceptor (DAAzo) pair, hence, the proximity relationship of the C_H2 domains, the fluorescence spectral properties of the normal rabbit IgG–AEDANS/anti-lactose–DAAzo (hybrid A) and normal rabbit IgG–AEDANS/anti-lactose–IAA (hybrid C) preparations were compared. For this, it was reasoned that if energy transfer were taking place between the donor and acceptor, the resultant quenching of the donor could be terminated by denaturing the protein, thereby eliminating the noncovalent interactions holding the two HL pairs together. The comparison of hybrids A and C in the presence of guanidine-HCl would allow the relative concentrations of AEDANS to be determined and corrections made for this factor.

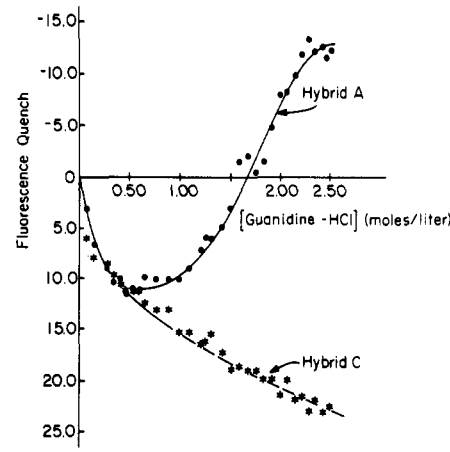

FIGURE 4: Comparison of the relative fluorescence intensity of hybrid A and hybrid C, with 330-nm excitation and 500-nm emission, is shown as a function of increasing concentrations of guanidine-HCl. Emission was corrected for dilution and solvent contribution. Negative quench represents an emission signal greater than the initial intensity.

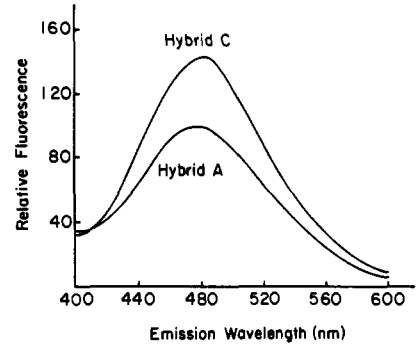

FIGURE 5: Relative uncorrected emission scans of hybrid A and hybrid C are shown. Excitation was at 330 nm with a 20-nm excitation slit and a 10-nm emission slit. Scans are the average of duplicate samples at approximately 4×10^{-7} M IgG. Scans were corrected for donor concentration by normalization to emission scans of the hybrid preparations in 4.0 M guanidine-HCl.

Figure 4 shows the effect of increasing concentrations of guanidine-HCl upon the emission of the two hybrid preparations. From 0 to 0.5 M guanidine–HCl, both preparations exhibited a similar reduction in fluorescence whereas from 1.0 to 2.5 M guanidine–HCl there was an enhancement of the emission for hybrid A only. This result is consistent with the existence of energy transfer quenching in hybrid A which is absent from hybrid C. The gradual decrease in the 500-nm emission of hybrid C with increasing concentrations of guanidine-HCl was due to a decrease in the quantum yield of the covalent probe. The difference in the emission characteristics of AEDANS–IgG in phosphate-buffered saline and in the denaturing solvent is attributed to a disruption of the tertiary structure of the hinge region, to which the AEDANS is adjacent.

Figure 5 shows a comparison of the relative emission spectra for both rabbit hybrid IgG preparations in phosphate-buffered saline, pH 7.2. The emission scans were corrected for differences in the concentration of the AEDANS donor by normalizing to the 490-nm emission of the respective hybrid preparation in a 4.0 M guanidine-HCl solvent. The transfer efficiency, E, was determined by eq 8 where Q_t and Q_o are

$$E = 1 - Q_t/Q_o \quad (8)$$

the quantum yields of hybrids A and C, respectively. If the

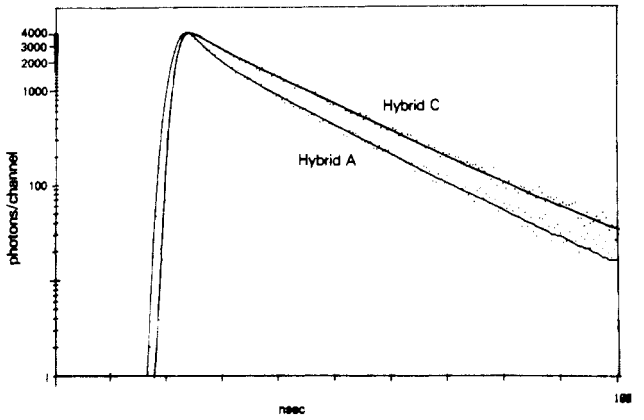

FIGURE 6: Excited-state decay kinetics of the covalently linked AEDANS fluorophore in rabbit noncovalent hybrid preparations. The exciting lamp flash passed through a 355 ± 40 nm filter, and the emitted photons were selected by a 455-nm cutoff filter. Data from the monophoton counting instrument are presented as photons per channel on a logarithmic scale. Each channel corresponds to 0.53 ns. Experimental data (···) were analyzed by the Laplace transform method (Gafni et al., 1975), using experimental profiles for the exciting lamp flash (not shown). The best fits of two-component decay curves for this particular run were obtained with the following parameters: for hybrid A, τ_L = 12.7 ns with amplitude 0.32 and τ_S = 2.2 ns with amplitude 0.68; for hybrid C, τ_L = 13.7 ns with amplitude 0.58 and τ_S = 2.5 ns with amplitude 0.42. The theoretical decay curves (—) were obtained by convolution of the two-component exponential decay with the experimental lamp profile for each hybrid. The data for hybrid C were normalized to the same peak height as those for hybrid A in order to facilitate visual comparison of the two curves. This procedure was the mathematical equivalent of counting photons for a shorter time during data acquisition and simply lowered the curve for hybrid C without changing its shape.

assumption were made that there was a uniform quenching for all donor–acceptor pairs, then an apparent distance of 48 Å could be calculated for R by using eq 6 and the observed values of 28.1% and 25.3% (average 26.7% ± 2.0%) for E.

Fluorescence decay curves were obtained by the monophoton counting method for each hybrid preparation (Figure 6). Both a short-lifetime (τ_S) component of 2–3 ns and a longer component (τ_L) with a decay time of 12.5–14 ns were observed. Long lifetimes of 14.0, 13.7, and 13.6 ns were calculated for three independent measurements of hybrid C (average 13.8 ± 0.2 ns). For hybrid A, long lifetimes of 12.6, 12.6, and 12.7 ns were observed (average 12.6 ± 0.1 ns).

The fluorescence decay data were also used to calculate the efficiency of energy transfer, E. When two lifetimes are required to characterize a sample, eq 8 becomes eq 9

$$E = 1 - \frac{\alpha_L\tau_L + \alpha_S\tau_S}{\alpha_L^0\tau_L^0 + \alpha_S^0\tau_S^0} \quad (9)$$

where the superscripted and nonsuperscripted parameters refer to measurements made on hybrids C and A, in the absence and presence of energy transfer, respectively. The amplitudes in both cases must also be normalized such that

$$\alpha_L + \alpha_S = \alpha_L^0 + \alpha_S^0 = 1 \quad (10)$$

The numerator and denominator in eq 9 are proportional to the total fluorescence intensity for the quenched and unquenched cases. For comparison, we also used only the long-lifetime component to calculate the efficiency of energy transfer from eq 11, which assumes a uniformity of the energy

$$E = 1 - \frac{\tau_L}{\tau_L^0} \quad (11)$$

transfer process, such that both the quenched and unquenched fluorescence can be characterized by a single-component decay.

Table I: Lifetime Analysis of Energy Transfer

	hybrid A	hybrid C
donor	AEDANS	AEDANS
acceptor	DAAzo	none
lifetime 1 (ns)[a]	12.6 ± 0.1	13.8 ± 0.2
amplitude 1	0.32 ± 0.1	0.55 ± 0.04
lifetime 2 (ns)	2.1 ± 0.1	2.6 ± 0.3
amplitude 2	0.68 ± 0.01	0.45 ± 0.04
E[b] (%)	38	
E_L[c] (%)	8.7	

[a] Lifetimes and amplitudes are the mean ± standard deviation for three independent measurements on each sample. [b] Efficiency of energy transfer as calculated from eq 9. [c] Efficiency of energy transfer as calculated from the change in the long lifetime only, eq 11.

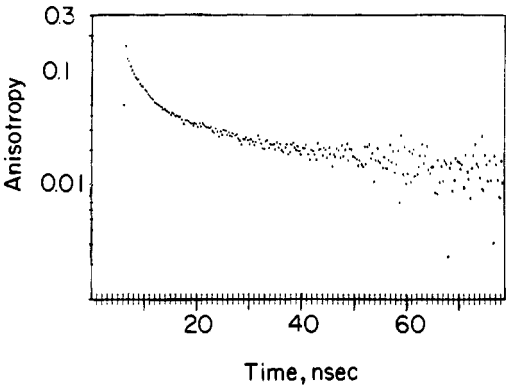

FIGURE 7: Time dependence of fluorescence anisotropy after a rapid exciting flash for IgG hybrid A. Nonpolarized exciting light was used, and vertically and horizontally polarized emitted light was measured as described under Materials and Methods. At each time, the anisotropy was calculated from the observed intensities according to eq 2 and 3.

The experimental values for the best two-component curves to fit the observed fluorescence decays of hybrids A and C are shown in Table I. The calculated efficiency (eq 9) was 38%. If only the long-lifetime component was used, a value for E of 8.7% was obtained (eq 11), corresponding to 48 Å. Both a relative increase in the intensity of the short-lifetime component as well as a decrease in the long-lifetime component of the donor were observed for the hybrid preparation in which an acceptor was present. Qualitatively, these effects can be seen in Figure 6 as a greater curvature in the fluorescence decay curve of hybrid A, as compared to that of the control. Clearly, the observed quenching of the donor emission was nonuniform.

Time-resolved emission anisotropy measurements showed extensive depolarization of the donor fluorophore within 2–3 ns after excitation, indicating that the donor possessed very rapid mobility independent of the slower rotation of the protein to which it was attached. The decay curve for hybrid A is shown in Figure 7. The curve for hybrid C was indistinguishable, as would be predicted for molecules having the same dimensions, by virtue of the mathematical definition of the anisotropy (Yguerabide, 1972). Anisotropy depends on the rotational properties of the sample and, unlike the fluorescence polarization, would be unaffected by the differences in the excited-state lifetimes in hybrids A and C. The long exponential decay time of the anisotropy was attributed to the rotation of the AEDANS/protein complex. From the slope of the curve in Figure 7 at long times, this rotation correlation time appeared to be 50–100 ns.

Two factors contributed to the rapid depolarization of the fluorescence emission. AEDANS had more than one excit-

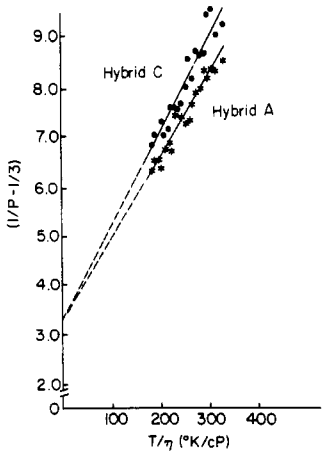

FIGURE 8: Steady-state, photon-counting fluorescence polarization of hybrid A and hybrid C as a function of absolute temperature (T) and viscosity (centipoise). Hybrid A (*): slope is 0.0165, P_0 is 0.275, and correlation coefficient for linear regression is 0.96. Hybrid C (●): slope is 0.0185, P_0 is 0.270, and correlation coefficient for linear regression is 0.95. Each point is the average of duplicates. Excitation wavelength is 330 nm, and emission wavelength is 500 nm.

ed-state dipole moment, which was shown by Hudson & Weber (1973) in studies of the steady-state poarization as a function of excitation wavelength. This factor would lead to a time-independent reduction in the emission anisotropy. We attribute to this the lowering of the observed initial anisotropy A to a value of approximately 0.13 from the theoretical value of 0.20 which would pertain for a single dipole. Extensive further depolarization was observed in the first 3–10 ns following the exciting flash, and this has been attributed to rapid rotational motion of the probe, independent of the protein to which it is anchored.

The initial rapid decrease of the anisotropy had a decay time of approximately 4–5 ns, as estimated from the slope of the curve in Figure 7 at very short times after the flash. The extent of the rapid depolarization can be described in terms of the wobbling-in-cone model where the donor is confined to a cone of half-angle θ (Kawato et al., 1978). The anisotropy A, after the decay due to rapid wobbling was virtually complete, and the initial value A_0 are related to the angle θ by the following equation:

$$A/A_0 = [0.5(1 + \cos\theta)\cos\theta]^2 \qquad (12)$$

From Figure 7, we obtained values of about 0.035 and 0.130 for A and A_0, respectively, which imply a cone half-angle of 50°.

Stryer (1978) has shown that this degree of rotation, on a time scale short in comparison with the excited-state lifetime, will tend to average the donor–acceptor orientations such that one can say with 90% certainty that distances which are calculated from observed energy transfer by assuming perfect randomness ($K^2 = 0.66$ in eq 7) will be in error by less than −10% to +20%. The averaging of orientations due to the rapid motion occurs in addition to that which results from multiple transition dipoles. From the analysis of Haas et al. (1978), the latter effect should, by itself, insure with 90% certainty that determinations of distances which are made by using $K^2 = {}^2/_3$ will be within 80–90% of the correct value.

A comparison of steady-state polarization, which depends upon both rotational mobility and the excited-state lifetime, of hybrids A and C as a function of the ratio of absolute temperature (T) to viscosity (η) is shown in Figure 8. The ratio of the effective excited-state lifetimes for the donor in the quenched vs. the unquenched state was inferred from the Perrin equation:

$$1/P - {}^1/_3 = (1/P_0 - {}^1/_3)\left(1 + \frac{R\tau}{V_0}\frac{T}{\eta}\right) \qquad (13)$$

Here, P is the fluorescence polarization (eq 1) and P_0 is its limiting value in the absence of rotation, R is the universal gas constant, V_0 is the equivalent sphere molar volume of the complex, and τ is the average lifetime of the excited state. For samples which were characterized by more than one lifetime, τ was a weighted average of the excited-state lifetimes of donors emitting photons. If the values for V_0 and P_0 were assumed to be identical for both hybrid preparations, the ratio τ/τ^0 obtained from steady-state polarization was equal to the ratio of the slopes of the plots of $1/P - {}^1/_3$ vs. T/η.

The assumption that V_0 was the same for both hybrid preparations was justified by the fact that these samples were chromatographed on the same Sephadex G-200 column under identical conditions to select the monomeric form of the four-chain structure. The samples were analyzed without further concentration, in order to minimize the possibility of forming soluble aggregates. The assumption was experimentally confirmed by the observed identity of the time-resolved emission anisotropy decay curves for the two hybrid preparations. The rationale for assuming that P_0 was the same for both preparations stemmed from the fact that the same starting material, normal rabbit IgG–AEDANS, was used to prepare both hybrid A and hybrid C. The AEDANS, therefore, must have been held within the same microenvironment for both samples, hence utilizing the same set of excited-state dipole moments. This latter assumption was also supported by direct evidence, since for the two samples the extrapolated values for P_0 were quite similar, i.e., 0.270 and 0.275. The true values for P_0 might have been slightly smaller than the extrapolated values, however, due to the independent rotational mobility of the fluorophore.

When the value for τ/τ^0 was inserted into eq 11, a value of 10.8% was obtained for the efficiency of energy transfer. The disparity between this value and the value of 26.7%, which was obtained from the quantum yield analysis, confirms that the complex weighted average lifetime derived from the polarization analysis was not identical with that derived from the quantum yield analysis. This disparity is another indication that the quenching of the donor excited-state lifetime by the acceptor was nonuniform.

Discussion

The experiments reported in this paper were designed to determine the effects of mild reduction and alkylation upon the quanternary structure of the IgG molecule. The resonance energy transfer technique was used to examine the intramolecular separation between the two alkylated Cys-242 residues which form the single hinge, inter-heavy-chain disulfide bond in the intact rabbit IgG molecule. Our analysis indicated a distribution of distances between the donor and acceptor probes.

There was a marked difference between the AEDANS fluorescence decay times in the hybrid preparations, which differed only by the presence or absence of an acceptor. The semilogarithmic graphs in Figure 6 show a pronounced increase in curvature, as well as the shorter lifetime one expects from any quenching process. The fluorescence decay clearly was not well characterized by a single lifetime. The observed complexity of the decay for the hybrid IgG preparation in which the acceptor was present was most likely due to intramolecular flexibility, which gave rise to a distribution of donor–acceptor distances. Such spatial nonuniformity would, in turn, give rise to a range of energy transfer efficiencies and,

therefore, to a range of fluorescence lifetimes.

Previous studies which have shown a similar correlation between donor–acceptor spatial nonuniformity and the loss of single-lifetime fluorescence decay include the following: Vanderkooi et al. (1973) measured the quenching of membrane-associated anthroylstearic acid by cytochrome *c*; Fung & Stryer (1978) monitored the energy transfer between fluorescent-labeled phospholipids in synthetic lipid vesicles as a function of increasing acceptor to donor ratios; Haas et al. (1978) studied a series of flexible oligopeptides which had a donor and acceptor at opposite ends. In contrast, Wu & Stryer (1972) described a system where the donor–acceptor separation was well-defined and found that the energy transfer process gave rise to a single fluorescence lifetime. In addition, these workers found excellent agreement for the single-lifetime quenching efficiencies measured by steady-state quantum yield analysis and monophoton lifetime analysis. In our study, the discrepancies between the nanosecond-resolved and steady-state measurements for mildly reduced and alkylated IgG indicated a range of lifetimes and consequently a range of distances in a segmentally flexible molecule.

We have analyzed our data to find the best two-exponential fit to the observed decay. This approach had the effect of mathematically identifying the long- and short-lived portions of the decay as separate components and assigning an average lifetime and a relative weight to each. The amplitudes, α_S and α_L, of the short- and long-lived components were proportional to the size of the fraction of the sample which radiated with decay times τ_S and τ_L, respectively. The products $\alpha_S\tau_S$ and $\alpha_L\tau_L$, on the other hand, were porportional to the total emission detected from each component. These products determined the extent of quenching that could be inferred from the lifetime analysis (eq 9). The most pronounced effect of the energy transfer process upon the observed fluorescence decay was the increase in the fraction of the sample whose radiation was detected in the short-lifetime component. This increase produced the increased curvature which can be seen in Figure 6. We attribute the greater curvature of the decay curve to the distribution of donor–acceptor separations at the moment of the exciting lamp flash. Therefore, the rate of donor quenching was not uniform.

The theoretical relationship between the rate of quenching and the distance between the donor and acceptor molecules is given by eq 4. This analysis cannot, however, be directly applied to a system in which the distance varies significantly from molecule to molecule. Since the energy transfer process has a nonlinear dependence on the separation, it would be simplistic to interpret the overall quenching in terms of an average donor–acceptor distance. However, from the lifetime measurements summarized in Table I, it is clear that for hybrid C 55% of the unquenched fluorophores emitted with long and 45% with short lifetimes (contributing 87% and 13% of the total emission, respectively). In contrast, only about 32% of the photons collected from the quenched sample, hybrid A, were in the long-lifetime component. We have calculated that this observation is algebraically consistent with 58% of the donor molecules being only slightly quenched (or unquenched) in the presence of the acceptor moiety and therefore continuing to contribute to the long-lived and short-lived components in a 55:45 ratio. The remaining 42% of the donor molecules in this model would be sufficiently quenched such that they would contribute only to the short-lifetime component.

Further experimental evidence confirming that the quenching was due to energy transfer was obtained from the polarization and anisotropy data. Since the Perrin equation (eq 13) predicts that the measured polarization of a sample depends on the fluorophore lifetime as well as on its characteristic time of rotation in solution, polarizations may be compared for two samples of the same molecular size and structure in order to detect a change in the fluorescence lifetime. The difference which was observed between the two hybrid molecules was not due to differences in rotational motion. This was shown by the fact that the time-dependent anisotropy, which is independent of the fluorescence lifetime, was identical for both hybrid preparations. The anisotropy decay curves made it clear, therefore, that the observed difference in steady-state polarization between the two samples was due solely to a difference in the excited-state lifetime of the AEDANS probe (Yguerabide, 1972).

In theory, the degree of donor quenching could be calculated from the measured steady-state polarization by utilizing the Perrin equation. The decrease in emission intensity in a uniformly quenched sample would not affect the measurement of its polarization. However, for the segmentally flexible IgG hybrid, the polarized emission was the sum of unequal contributions from various molecules. Each would exhibit different degress of quenching, depending on the donor–acceptor distance. Consequently, the observed polarization was a complex weighted average. In contrast, the quantum yield data on the same sample can be thought of as a simple average since the emissions from various molecules added together to give the total emission.

The discrepancy between the efficiencies of energy transfer inferren from quantum yield and polarization data was a further indication that the molecules of the sample were not uniformly quenched. On the one hand, we found a 27% efficiency of energy transfer by analyzing our quantum yield data as if the samples could be characterized by a single lifetime. On the other hand, the polarization data were influenced by the larger contributions from the least quenched molecules, and an apparent efficiency of only 11% was calculated from those data.

On the basis of the observed change in donor quantum yield and excited-state long lifetime as a consequence of energy transfer, we conclude that the majority of the mildly reduced and alkylated hybrid IgG molecules in solution were characterized by hinge regions which were separated by 50–60 Å. In the native molecule, however, the hinge regions are known to be held in close proximity by the hinge disulfide. In addition, the hinge disulfide can efficiency re-form after reduction. There must be a region within the Fc segment, therefore, which permits intramolecular flexibility. We suggest two possibilities which are not mutually exclusive.

In the first model, the secondary and tertiary structural elements of the C_H2 domains are maintained. This assumption is supported by the previsouly discussed circular dichroism and optical rotatory dispersion studies (Bjork & Tanford, 1971; Stevenson & Dorrington, 1970; Azuma et al., 1974). X-ray diffraction and biochemical analysis indicate strong trans noncovalent interactions between the C_H3, but not the C_H2, domains. Therefore, the switch region peptides which link C_H2 to C_H3 are a possible site of flexibility.

The second possibility is that the secondary and tertiary structure of the C_H2 domain is not rigorously maintained after mild reduction and alkylation. Individual strands of the β-pleated sheets might attain some degree of mobility independent of other strands of the domain. This model is supported by hydrogen exchange experiments previously discussed (Venyaminov et al., 1976). Both models imply that neither the cis noncovalent interactions between C_H2 and C_H3 nor the

trans noncovalent interactions between adjacent C_H2 domains are strong enough to sustain the rigidity of the Fc segment in the absence of the hinge disulfide bond.

The question can then be asked whether the change in the configuration of the IgG molecule, as a consequence of mild reduction and alkylation, is responsible for the concomitant attenuation of Fc effector functions. This question is particularly relevant to the binding and activation of the C1q component of complement because of the involvement of the C_H2 domain. The controversy of whether or not a conformational change is a prerequisite to the activation of complement by IgG bound to antigen can be bypassed if the discussion is initially limited to the binding of C1q to free IgG (Metzger, 1974, 1978).

It seems unlikely that C1q binding is dependent upon the quaternary structure of the $C\gamma2$ module. Although C1q binding to free IgG could be eliminated by mild reduction and alkylation, the binding to free Fc or free C_H2 was shown not to be dependent upon the integrity of the interchain disulfide bond (Isenman et al., 1975; Yasmeen et al., 1976). These findings led to the hypothesis that C1q binding to reduced and alkylated IgG was prevented by the increased segmental flexibility of the Fab segments which sterically hindered C1q binding. This hypothesis was supported by the observation that the Fc fragment from human IgG4 binds C1 while the intact molecule does not. It should be noted that the comparison of segmental flexibility of native and mildly reduced rabbit IgG by nanosecond emission anisotropy analysis indicated that the angular range which the Fab segment was permitted to traverse had increased due to mild reduction (Chan & Cathou, 1977; Cathou, 1978). That analysis, however, was unable to define specifically a change in the relative positions of the Fab segment and the C_H2 domain, where the C1q binding site is located.

Alternatively, mild reduction and alkylation could destabilize the C1q binding site located within the C_H2 domain. Increased instability or flexibility of the tertiary structural elements could serve to decrease the change in free energy associated with the C_H2–C1q interaction. The comparison of the binding of pancreatic trypsin inhibitor (PTI) to trypsin and trypsinogen serves as a prototype. The structure of trypsin and its interaction with PTI are characterized by an association constant of 10^{13} M^{-1} and have been analyzed in X-ray crystallographic studies. X-ray diffraction analysis of trypsinogen indicated that 85% of its tertiary structure was identical with that of trypsin. The remaining 15%, including the PTI binding site, showed no significant electron density in the electron density map, a finding which indicated flexibility of the secondary and tertiary structure. Upon binding PTI, trypsinogen adopted a trypsinlike conformation in which the activation domain became rigid. The association constant for the trypsinogen–PTI interaction was 5×10^5 M^{-1}, indicating that a major portion of the free energy of binding was allocated to the rigidification of the zymogen (Felhammer et al., 1977; Bode et al., 1978; Bode, 1979).

Evidence for structural instability of reduced and alkylated IgG has been reported by Venyaminov and co-workers (1976) in a study which compared the kinetics of hydrogen–deuterium exchange for native and mildly reduced and alkylated human IgG1. They concluded that the modified protein possessed increased conformational mobility accompanied by extensive destabilization of protein conformation affecting 90% of the peptide groups covered by their measurements. The authors suggested that tensile or stretching forces exerted by the Fab segments increased the probability of solvent exposure for slow-exchanging, hydrogen-bonded peptides of the Fc segment. The ability of C1q to bind the mildly reduced and alkylated Fc fragment but not to bind reduced IgG may be the consequence of a C_H2 domain destabilization by Fab tensile forces. The activation of the classical complement pathway by antigen-bound IgG may be, however, more complex than the binding of C1q to antigen–antibody complexes. The biological significance of observed conformational changes in the antibody molecule as a function of binding antigen is at present unclear (Schlessinger et al., 1975; Vuk-Pavlović et al., 1978).

In conclusion, on the basis of our energy transfer analysis, we propose that as a consequence of mild reduction and alkylation the rabbit IgG molecule is no longer in a native configuration. In the native molecule, the hinge regions are known to be inclose proximity because they are covalently linked by a disulfide bond. Our analysis indicates that in the absence of the hinge disulfide bond the hinge regions are separated by a distribution of distances, and for the majority of the molecules in solution (~60%) the separation is 50–60 Å. In the context of current knowledge of the IgG molecule derived from biochemical and X-ray diffraction analysis, it is evident that the principle forces maintaining the integrity of the native, functional Fc segment of the rabbit IgG molecule are the strong noncovalent interactions of the C_H3 domains and the single inter-heavy-chain hinge disulfide linkage.

Acknowledgments

We are indebted to Dana Wontorsky for the preparation of the vaccine, to George Woodrow III for the computer programs used in the analysis of the anisotropy measurements and fluorescence decay, and to Sally Karush for the meticulous preparation of the manuscript.

References

Arend, W. P., & Mannik, M. (1972) *J. Exp. Med. 136*, 514–530.

Azuma, T., Hamaguchig, K., & Migita, A. (1974) *J. Biochem. (Tokyo) 76*, 685–693.

Bjork, I., & Tanford, C. (1971) *Biochemistry 10*, 1289–1295.

Bode, W. (1979) *J. Mol. Biol. 127*, 357–374.

Bode, W., Schwager, P., & Huber, R. (1978) *J. Mol. Biol. 118*, 99–112.

Cathou, R. E. (1978) *Compr. Immunol. 5*, 37–83.

Chan, L. M., & Cathou, R. E. (1977) *J. Mol. Biol. 112*, 653–656.

Davies, D. R., Padlan, E. A., & Segal, D. M. (1975) *Annu. Rev. Biochem. 144*, 639–667.

Deisenhofer, J., Colman, P. M., Huber, R., Haupt, H., & Schwick, G. (1976) *Hoppe-Seyler's Z. Physiol. Chem. 357*, 435–445.

Dorrington, K. J. (1978) *Can. J. Biochem. 56*, 1087–1101.

Felhammer, H., Bode, W., & Huber, R. (1977) *J. Mol. Biol. 111*, 415–438.

Fruchter, R. G., Jackson, S. A., Mole, L. E., & Porter, R. R. (1970) *Biochem. J. 116*, 249–259.

Fung, B. K., & Stryer, L. (1978) *Biochemistry 17*, 5241–5248.

Gafni, A., Modlin, R. L., & Brand, L. (1975) *Biophys. J. 15*, 263–280.

Ghose, A. C., & Karush, F. (1973) *Biochemistry 12*, 2437–2443.

Haas, E., Katchalski-Katzir, E., & Steinberg, I. Z. (1978) *Biochemistry 17*, 5064–5070.

Hong, R., & Nisonoff, A. (1965) *J. Biol. Chem. 240*, 3883–3891.

Hudson, E. N., & Weber, G. (1973) *Biochemistry 12*, 4154–4160.

Isenman, D. E., Dorrington, K. J., & Painter, R. H. (1975) *J. Immunol. 114*, 1726–1729.
Kabat, E. A., Wu, T. T., & Bilofsky, H. (1979) NIH Publication No. 80-2008, Bethesda, MD.
Kawato, S., Kinosita, K., Jr., & Ikegami, A. (1978) *Biochemistry 17*, 5026–5031.
Luedtke, R., Owen, C. S., & Karush, F. (1980) *Biochemistry 19*, 1182–1192.
Means, G. E., & Feeney, R. E. (1971) in *Chemical Modification of Proteins*, Chapter 6, pp 105–110, Holden-Day, San Francisco, CA.
Metzger, H. (1974) *Adv. Immunol. 18*, 169–207.
Metzger, H. (1978) *Contemp. Top. Mol. Immunol. 7*, 119–152.
Michaelsen, Y. E., Wisloff, F., & Natvig, J. B. (1975) *Scand. J. Immunol. 4*, 71–78.
Parker, C. W., Yoo, T. J., Johnson, M. C., & Godt, S. M. (1967) *Biochemistry 6*, 3408–3416.
Poljak, R. J. (1975) *Nature (London) 256*, 373–376.
Rockey, J. H., Montgomery, P. C., Underdown, B. J., & Dorrington, K. J. (1972) *Biochemistry 11*, 3172–3181.
Romans, D. G., Tilley, C. A., Crokkston, M. C., Falk, R. E., & Dorrington, K. J. (1977) *Proc. Natl. Acad. Sci. U.S.A. 74*, 2531–2535.
Sakano, H., Rogers, J. H., Hüppi, K., Brock, C., Traunecher, A., Maki, R., Wall, R., & Tonegawa, S. (1979) *Nature (London) 277*, 627–633.
Schlessinger, J., Steinberg, I. Z., Givol, D., Hochman, J., & Pecht, I. (1975) *Proc. Natl. Acad. Sci. U.S.A. 72*, 2775–2779.
Stevenson, G. T., & Dorrington, K. J. (1970) *Biochem. J. 118*, 703–712.
Stryer, L. (1978) *Annu. Rev. Biochem. 47*, 819–846.
Vanderkooi, J., Erecińska, M., & Chance, B. (1973) *Arch. Biochem. Biophys. 154*, 219–229.
Van Der Meulen, J. A., McNabb, T. C., Haeffner-Cavaillon, N., Klein, M., & Dorrington, K. J. (1980) *J. Immunol. 124*, 500–507.
Venyaminov, S. Y., Rajnavölgyi, E., Medgyesi, G. A., Gergely, J., & Zavodsky, P. (1976) *Eur. J. Biochem. 67*, 81–86.
Vuk-Pavlović, S., Blatt, Y., Glaudemans, C. P. J., Lancet, D., & Pecht, I. (1978) *Biophys. J. 24*, 161–174.
Wahl, P. (1975) *Biochem. Fluoresc. Concepts 1*, 1–41.
Wu, C., & Stryer, L. (1972) *Proc. Natl. Acad. Sci. U.S.A. 69*, 1104–1108.
Yasmeen, D., Ellerson, J. R., Dorrington, K. J., & Painter, R. H. (1976) *J. Immunol. 116*, 518–527.
Yguerabide, J. (1972) *Methods Enzymol. 26*, 498–577.

Role of Tryptophanyl and Tyrosyl Residues of Flavoproteins in Binding with Flavin Coenzymes. X-ray Structural Studies Using Model Complexes†

Masatoshi Inoue, Megumi Shibata, Yu-ichi Kondo, and Toshimasa Ishida*

ABSTRACT: The crystal structures of 7,8-dimethylisoalloxazine-10-acetic acid–tryptamine (1:1) tetrahydrate and 7,8-dimethylisoalloxazine-10-acetic acid–tyramine (1:1) tetrahydrate complexes were determined by the X-ray diffraction method, as models for flavin–tryptophan and flavin–tyrosine interactions in flavoproteins. The observed parallel stackings and the intermolecular spacing distances, which were less than the normal van der Waals separation between the isoalloxazine and indole rings and between the isoalloxazine and phenol rings, suggest the existence of charge-transfer interactions in their ground states. The indole and phenol rings interact with the pyrimidinoid and pyrazinoid portions of the isoalloxazine ring and have short contacts, <3.4 Å, with the reduction site (N1 and N5 atoms) of this ring. This suggests that the reduction of oxidized flavin to the semiquinone state may be facilitated by charge transfer from the former rings to the N1 and N5 atoms. Absorption difference spectra showed that both complexes associate with equimolar ratios in solution as well as in the crystalline state and that they have the same charge-transfer bands and association constants as flavin mononucleotide (FMN)–Trp and FMN–Tyr complexes, respectively. On the other hand, proton magnetic resonance spectra suggested that in solution, the stacking modes of the indole and phenol rings to the isoalloxazine ring are different from those observed in the crystal structures and both aromatic rings are stacked over the whole of the isoalloxazine ring.

In living cells, flavoprotein require flavins such as FMN[1] and FAD for effective oxidation–reduction catalyses. For an understanding of the mechanism of action of flavoproteins, which are formed via a simple biomolecular process, i.e., apoprotein + flavin ⇌ flavoprotein, the details of the flavin–apoprotein interaction need to be elucidated. Information gained by diverse spectral studies of native and chemically modified flavoproteins, augmented by X-ray crystallography, provides unequivocal evidence for the interaction of the flavin isoalloxazine ring with aromatic amino residues within the flavin-binding sites of numerous flavoproteins [for reviews, see Mayhew & Ludwig (1975) and McCormick (1977)]. For instance, X-ray studies on flavodoxin from *Desulfovibrio vulgaris* (Watenpaugh et al., 1973) showed that Trp-60 and Tyr-99 residues are involved in cofactor binding with FMN. Table I lists the some flavoproteins in which the aromatic amino acid participates in the binding with flavin; obviously,

† From the Department of Physical Chemistry, Osaka College of Pharmacy, 2-10-65 Kawai, Matsubara-City, Osaka 580, Japan. *Received October 24, 1980.* This work is part VII of "Structural Studies of the Interaction between Indole Derivatives and Biologically Important Aromatic Compounds". Reference Ishida et al. (1980) is an earlier study in this series.

[1] Abbreviations used: DIA, 7,8-dimethylisoalloxazine-10-acetic acid; TPA, tryptamine; TRA, tyramine; DSS, 2,2-dimethyl-2-silapentane-5-sulfonate; PMR, proton magnetic resonance; CNDO/2, complete neglect of differential overlap; FMN, flavin mononucleotide; FAD, flavin adenine dinucleotide.

0006-2960/81/0420-2936$01.25/0